Water Science & Technology | 68.1 | 2013

Experimental study of the performance of a siphon sediment cleansing set in a CSO chamber

Yongchao Zhou, Yiping Zhang, Ping Tang, Yongmin Chen and David Z. Zhu

ABSTRACT

Model experiments were conducted to investigate the performance of a siphon sediment cleansing set (SSCS) for preventing sediment deposition on the combined sewer overflow (CSO) chamber bottom. The results confirmed the effectiveness of siphon suction in sediment removal in the chamber. The sediment scour test revealed that the equilibrium scour depth correlated significantly with the siphon-lift capacity of the SSCS, which was a function of the initial siphon head and the cross-sectional area ratio between the CSO chamber and the siphon.

Key words | bed shear stress, CSO chamber, hydraulic performance, sediment cleansing, sediment scour

Yongchao Zhou
Yongmin Chen
College of Civil Engineering and Architecture,
Zhejiang University,
A810 Anzhong Building, Hangzhou, 310058,
China

Yiping Zhang (corresponding author)
College of Civil Engineering and Architecture,
Zhejiang University,
A505 Anzhong Building, Hangzhou, 310058,
China
E-mail: *zhangyiping@zju.edu.cn*

Ping Tang
College of Environment and Material Engineering,
Hangzhou Dianzi University, Hangzhou, 310027,
China

David Z. Zhu
Department of Civil and Environmental Engineering,
University of Alberta, Edmonton, AB,
Canada T6G 2W2

INTRODUCTION

In combined sewer systems, during wet weather, the total flows can exceed the capacity of the intercepting sewer system or the treatment plant. The excess flow is then discharged to the receiving water through combined sewer overflow (CSO) chambers. A CSO typically carries a high partition of pollutants and causes harmful impacts on the environment (Ashley *et al*. 2004). In addition, the sediment deposition in the system may cause operational problems, such as loss of hydraulic capacity, in-pipe septicity and contribution to the pollutants in foul flushes (Ashley *et al*. 2000). A number of studies have been conducted on hydraulic performance and/or sediment retention efficiency of CSO chambers by physical laboratory modeling and computational fluid dynamics modeling (Stovin & Saul 2000; Harwood & Saul 2001; Dufresne *et al*. 2009). Recently significant attention has been drawn to sediment control and management in sewer systems. Several techniques for the removal of sediment deposits from sewer systems have been developed using different mechanical and hydraulic devices (Chebbo *et al*. 1996; Pisano *et al*. 1998; Bertrand-Krajewski 2003). In particular, a few studies (Bertrand-Krajewski 2003; Pisano *et al.* 2003; Bertrand-Krajewski *et al.* 2004; Campisano *et al.* 2006, 2007, 2008) focused on the use of flushing devices. Among them, Campisano *et al.* (2006, 2007, 2008) studied sediment scour effectiveness and the design of flushing devices. Such devices can produce successive flushing waves with high flow velocities and shear stresses to scour and transport the sediments deposited on the collector bottom.

In Liuzhou, China, the combined sewer outlets near the bank of Liujiang River are typically buried over 10 m below the ground. In order to reduce the project cost, the main intercepting sewers were constructed at much higher elevations than the combined sewer channels. Therefore, one specific CSO chamber was adopted in the combined sewer system as shown in Figure 1. The water level in the upstream of the combined sewer channel was lifted by the high weir in the CSO chamber, even in dry weather, and the wastewater was conveyed in the condition of pressurized flow as shown in Figure 1(a). The intercepting dry

doi: 10.2166/wst.2013.238

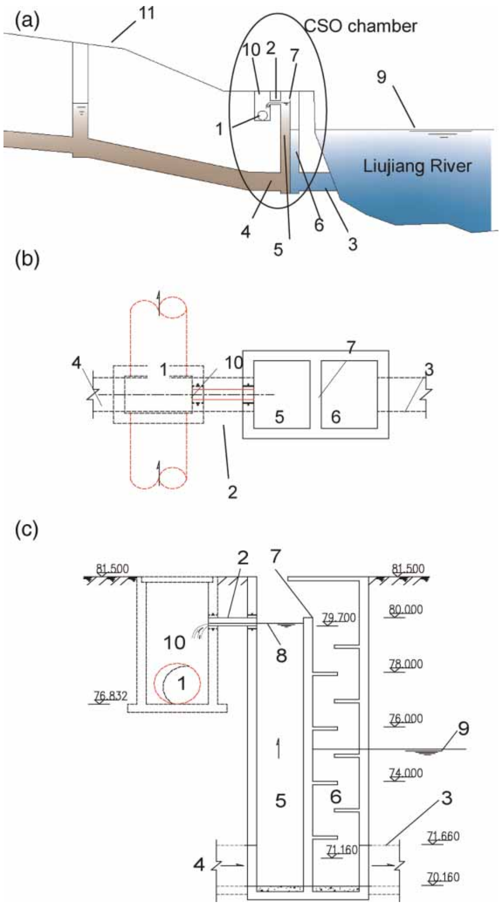

Figure 1 | The deep CSO chamber in the intercepting sewer system in Liuzhou, China. (a) Panorama; (b) plan view; (c) cross-section view with the installation of SSCS. 1. main intercepting sewer; 2. branch intercepting sewer; 3. combined sewer outlet; 4. combined sewer channel; 5. overflow chamber; 6. discharge chamber; 7. weir; 8. intercepting water level; 9. water level of receiving water; 10. intercepting chamber; 11 ground.

wastewater flows up to the intercepting chamber through the branch intercepting sewer. When the storm water runoff exceeds the intercepting capacity, the excess water flows over the weir to the discharge chamber and discharges through the combined sewer outlets into the receiving waters. The sediment deposits easily on the bottom of the overflow chamber in dry weather. Hence, a siphon sediment cleansing set (SSCS) was designed to clear the sediment on the chamber bottom in dry weather as shown in Figure 2(a). The SSCS was installed in the chamber, which can convert small, continuous flows into large, intermittent pulse flows.

Siphon-lift technologies have been used in dredging reservoir deposits for decades. The suction pressure and velocity under the condition of the different suction heads and distance to reservoir bed were investigated by Chen *et al.* (2010). However, there has been little work about the siphon suction in a finite chamber and its effect on sediment removal. The present study was undertaken to improve our understanding of hydraulic behaviors in the bottom of the overflow chamber with the SSCS, as well as its effect on sediment erosion and removal.

EXPERIMENTAL INVESTIGATION

A model CSO chamber was built at Zhejiang University at a scale of 1:5, as shown in Figure 1. The experimental setup was made up of a 1.0 m high CSO chamber, and a 1.8 m long rectangular flume with an upstream sewer junction and a circulating cistern. The rectangular flume, the model combined sewer, had a cross-section 0.2 m wide and 0.2 m deep and a longitudinal slope of 0.1%. The upstream sewer junction chamber was a rectangular box of 0.5 m × 0.5 m × 1.0 m (length × width × height). The model CSO chamber also consisted of the overflow chamber 0.3 m long, 0.5 m wide and 1.1 m high; intercepting chamber 0.2 m long, 0.5 m wide and 1.1 m high; as well as the outlet chamber 0.2 m long, 0.5 m wide and 0.6 m high. The pipe diameters of the combined sewer outlet and intercepting sewer were 200 mm.

As shown in Figure 2(a), the water level in the overflow chamber and siphon pipe of the SSCS rose slowly with the inflow from the rectangular flume. Just before it reached the top of the siphon pipe turn, water entered the auxiliary siphon pipe, whereby the fall of water caused the air to evacuate from the siphon via the air evacuation pipe, thus starting the siphon action. When the water level in the overflow chamber decreased to the siphon-breaking hole level, the siphon process would break. The periodic siphon suction forms automatically with the siphon forming and breaking processes.

Three model SSCSs with flow cross-section dimensions of 50 mm × 55 mm, 50 mm × 100 mm, 50 mm × 200 mm were applied, combined with several downstream boundary conditions (weir heights) in the tests. Let S be the area ratio between the flow section area of the SSCS (Figure 2(b)) and the bottom of the overflow chamber, then S equals 0.0275, 0.05 and 0.1. The initial siphon head (h), shown in Figure 2, can be adjusted through the water level in the intercepting chamber by an adjustable weir plate; $h = 0.75$, 0.60, 0.45 and 0.30 m in the tests.

The first set of experiments was developed without sediments in order to investigate the hydraulic behavior. The velocity fields in the overflow chamber were measured

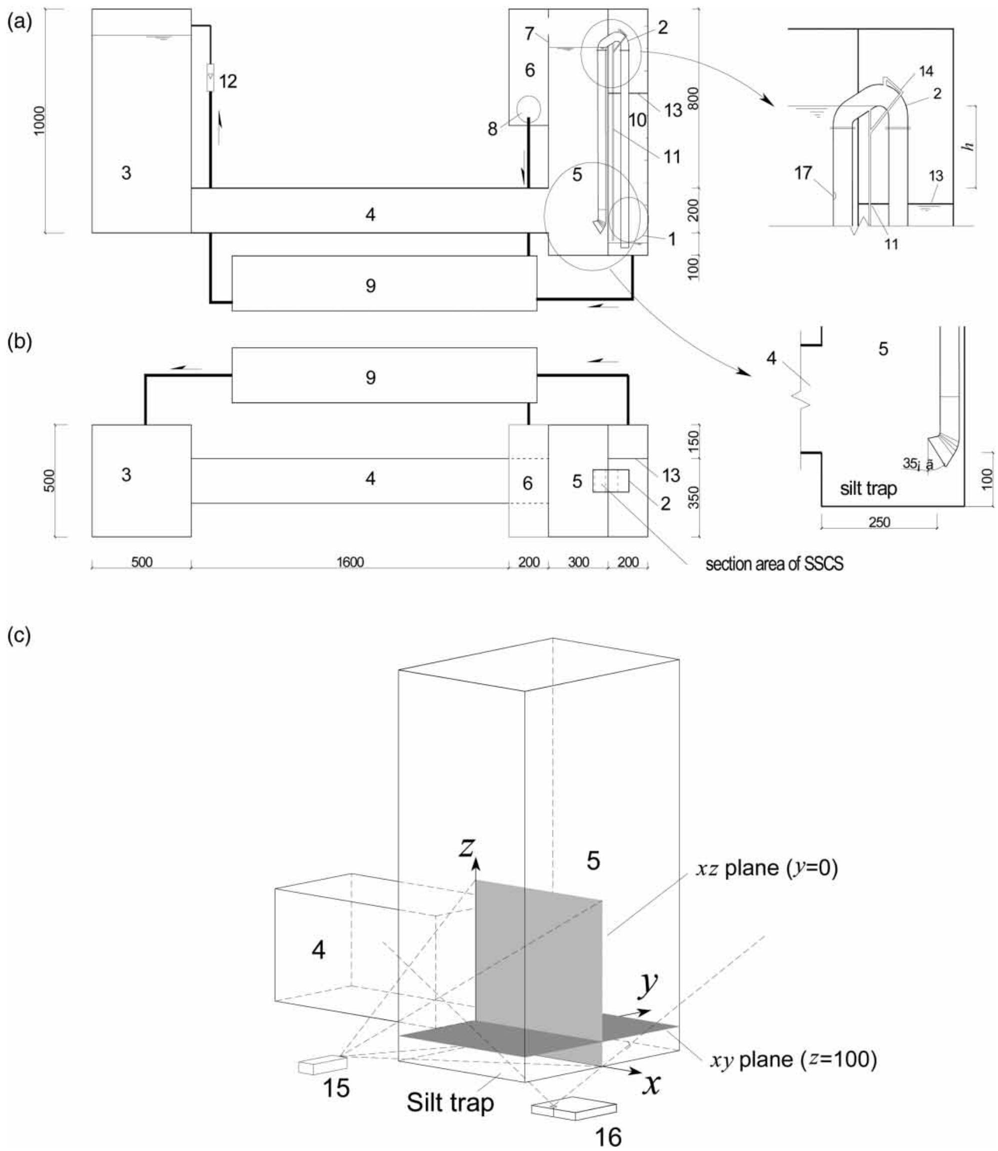

Figure 2 | The sections (a) and plans (b) of experimental setup in the overflow chamber (c). (Note that the intercepting chamber is placed to the right of the overflow chamber in the laboratory model.) 1. intercepting sewer; 2. self-siphon sediment cleansing set; 3. the upstream combined sewer junction; 4. rectangular flume (combined sewer); 5. overflow chamber; 6. discharge chamber; 7. overflow weir; 8. combined sewer outlet; 9. a circulating cistern; 10. intercepting chamber; 11. auxiliary siphon pipe; 12. flow meter; 13. adjustable weir plate; 14. air exhaust pipe of self-siphon set; 15. camera; 16. laser sheet; 17. siphon-breaking hole.

using the Dantec PIV (particle image velocimetry) system (Dantec Dynamics) and flow manager software. The coordinate system, the primary planes and the experimental arrangement of PIV in the study of the overflow chamber is shown in Figure 2(c).

The second set of experiments was carried out with the sediments. Phenolic powder was used as non-cohesive sediment in the tests. According to the similarity theory, the specific gravity of the model sediment is 1,450 kg/m^3, and its mean effective grain diameter is 0.105 mm. The model sediment was built up to a deposit bed 100 mm thick in the silt trap initially. Water was taken from a public water supply tap in the laboratory and not recycled.

EXPERIMENTAL RESULTS AND DISCUSSION

Velocity distributions

During the siphon cycle, the instantaneous velocity changed with the changing water head; peak velocities (of up to 0.17 m/s ($S = 0.05$)) were obtained approximately 5 s after the start of the cycle. Velocities then dropped steadily as the cycle completed. Therefore, the time-averaged velocity vector fields were calculated by post-processing. The time-averaged velocity fields in the *xz*-plane at different longitudinal level of the overflow chamber with different SSCS and h appeared to be pretty much alike, and Figure 3 shows the velocity field with $S = 0.0275$ and $h = 0.75$ m. It can be seen from Figure 3(a) and (b) that flow was sucked into the sediment cleansing set directly after entering the chamber in the siphon inlet sections (in the *xz*-plane with $y = 0$ and $y = 50$ mm). Because the suction flow was greater than the discharge from the combined sewer, the water level in the upper part of the chamber dropped, and the downward flow was observed in the *xz*-plane with $y = 150$ mm and $y = 200$ mm (Figure 3(c),(d)). Therefore, the overall improvement in flow in the chamber can be achieved by siphon suction. The vertical distribution of time-averaged velocity also confirms the improvement. Taking the *xz*-plane with $y = 0$ (Figure 2(c)), for instance, the vertical distribution of time-averaged velocity in the plane on the bottom of chamber under different h is presented in Figure 4.

As shown in Figure 4, the velocity distribution increased significantly as the point approached the suction head of the SSCS. As the horizontal distance between the measurement point and the suction head increased, the velocity decreased rapidly at first and then stabilized gradually, which was quite different from the velocity distribution of suction in infinite water (Chen *et al.* 2010). It is helpful to have a finite size chamber for sediment cleansing by siphon suction.

The bed shear stress distributions

The bed shear stress (BSS) is more important than velocity vectors for evaluating the sediment erosion and re-suspension. From the PIV measurements, it is possible to estimate the BSS. The PIV measures two orthogonal

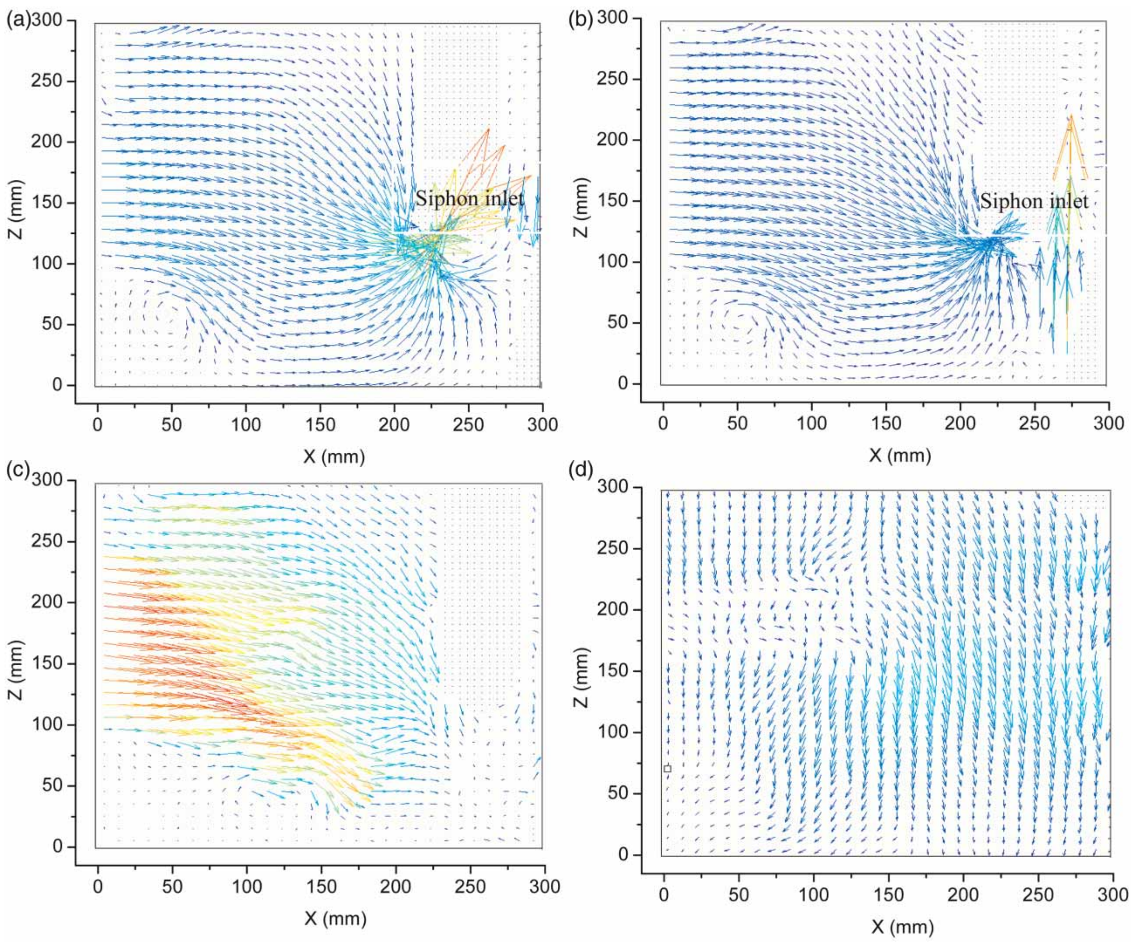

Figure 3 | Time-averaged velocity fields on the bottom of the overflow chamber with siphon sediment cleansing set ((a) $y = 0$, (b) $y = 50$, (c) $y = 100$, (d) $y = 150$).

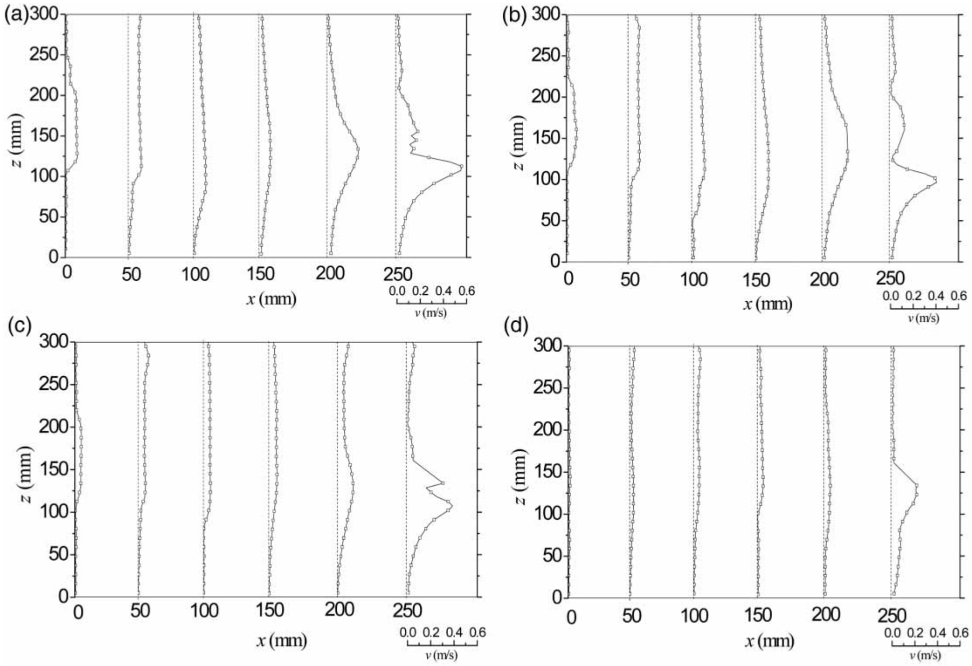

Figure 4 | The vertical distribution of time-averaged velocity in the *xz*-plane ($y = 0$) with $h = 0.75$ m (a), 0.60 m (b), 0.45 m (c) and 0.30 m (d).

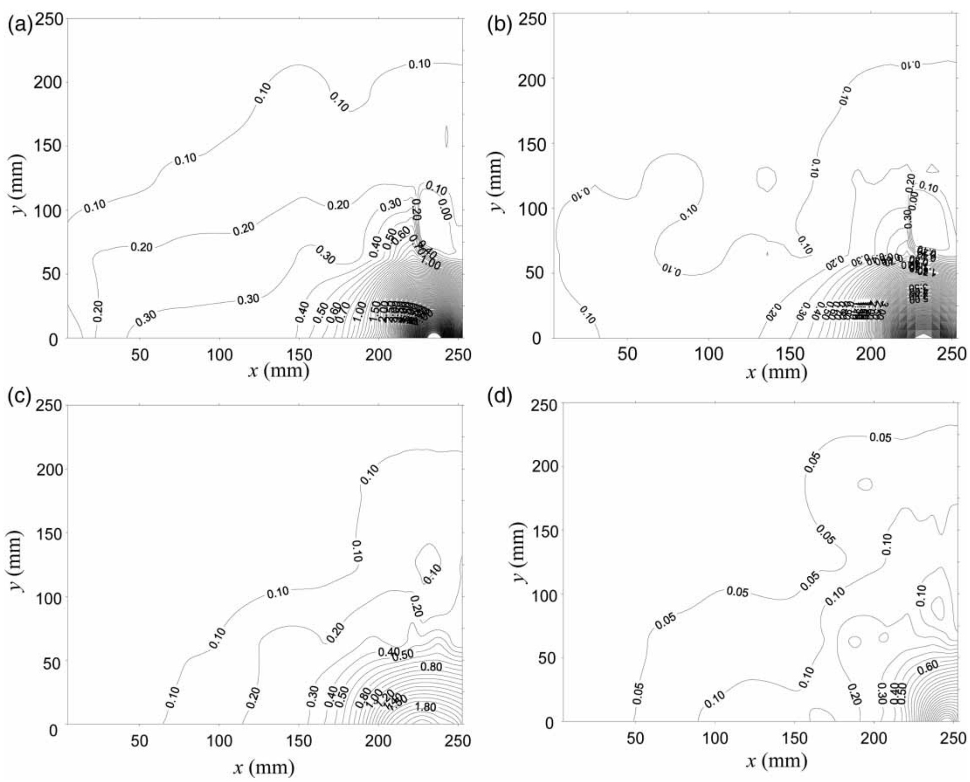

Figure 5 | The bed shear stress (*xy*-plane, $z = 0$ mm) of the overflow chamber with SSCS under a different water head (a) 0.75 m, (b) 0.60 m, (c) 0.45 m, (d) 0.30 m.

velocity vectors V_x and V_z in the streamwise and vertical directions, respectively. The BSS τ_o is estimated using

$$\tau_o = -\rho\overline{u'w'} \tag{1}$$

where $u' = V_x - \overline{V_x}$ and $w' = V_z - \overline{V_z}$; $\overline{V_x}$ and $\overline{V_z}$ are time-averaged velocity vectors in the streamwise and vertical directions.

Figure 5 shows the BSS distribution on the bottom (*xy*-plane, $z = 100$ mm and $y \geq 0$ mm due to symmetry) of the overflow chamber with SSCS (50 mm × 55 mm) under different *h*. As shown in Figure 5, the BSS was a minimum at every side, and increased from 0.05–0.1 N/m^2 to 2.0–8.0 N/m^2 with increasing longitudinal and lateral distance according to the value of *h*, and reached a peak near the suction head. The BSS in most of the surface reached 0.1–1.0 N/m^2 when $h = 0.75$ m. Ahyerre *et al.* (2001) investigated that the sediment layer with heavy pollutant loading in sewer is located at points where the BSS is <0.1 N/m^2; thus this layer can be easily removed by the SSCS. Moreover, it can be seen from Figure 5 that the parameter *h* was a sensitive factor to the shear stress distribution.

Scour in the bottom

Figure 6 shows the averaged scour depths in the bottom of the overflow chamber after several siphon suctions and the final equilibrium sediment surface shape under different *S*. The averaged scour depths were the greatest at the first suction and then stabilized to equilibrium at next suctions as shown in Figure 6(a). Due to the stronger suction-lift capacity of the SSCS with *S* of 0.05 and 0.1, the sediment layer reached an equilibrium state immediately after the first suction. Such an equilibrium could determine the sediment removal efficiency of different SSCSs. From Figure 6(b)–(d), the sediment equilibrium surfaces appeared similar in shape. It was found that the maximum scour depth occurred near the suction head and the minimum appeared on the four corners of the chamber. It was consistent with the distribution of the shear stress on the *xy*-plane (Figure 5). Moreover, the equilibrium scour depth was correlated significantly with the siphon-lift capacity of the SSCS. A larger siphon-lift capacity resulted in a deeper sediment scour. On the other hand, it was found from Figure 6 that the equilibrium sediment depth under a suction head decreased greatly at first and then became stable at

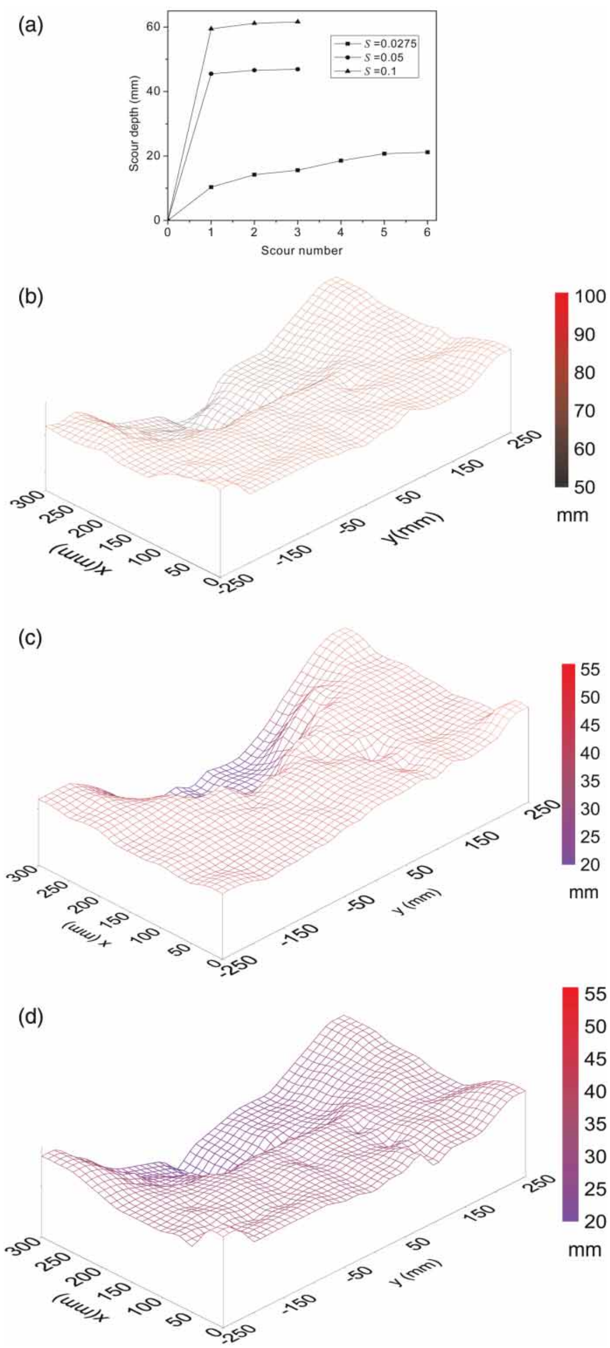

Figure 6 | The averaged scour depths on the bottom of the overflow chamber (a) and equilibrium sediment surface shape on the bottom as $S = 0.0275$ (b), 0.05 (c) and 0.1 (d).

about 20 mm when *S* increased from 0.0275 to 0.1, which was related to the fast attenuation of shear stress distribution in the vertical direction. It can be concluded that the siphon-lift capacity is the key to sediment removal; however, great improvement in sediment removal cannot be achieved only by enlarging the

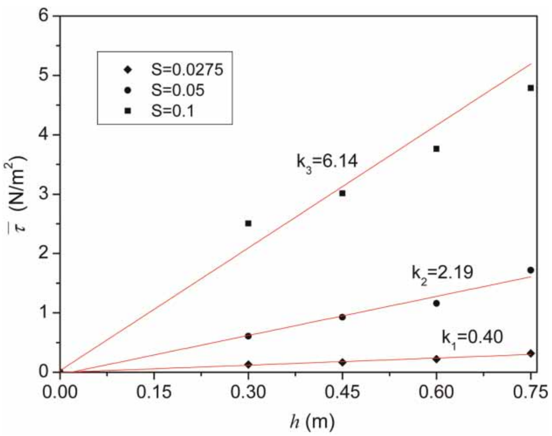

Figure 7 | The relationship between $\bar{\tau}$ and h for different S.

siphon-lift capacity. The suction head type, installation angle and height of SSCS should be studied further in order to improve sediment removal.

The siphon-lift capacity of the SSCS can be expressed by the weighted mean value of BSS ($\bar{\tau}$) on the bottom of the overflow chamber, which was affected by the value of h and S. The value of $\bar{\tau}$ for different h and S was plotted in Figure 7. A straight line was fitted to the data for the same S value. Figure 7 represents the linear relationships between $\bar{\tau}$ and h, and the relationships were obvious with goodness of fit (r^2)= 0.97, 0.97 and 0.98 respectively. The slopes of the lines (k) are 0.40, 2.19 and 6.14 and intercepts are almost zero, which explained physically that $\bar{\tau}$ would be zero when $h = 0$.

Our current understanding of the erosion and transport of sewer sediment is limited. Field studies have indicated a wide variability, both temporally and spatially, in the recorded values of sewer sediment critical shear stress. These values range from 0.7 to 7.0 N/m^2 (Skipworth *et al.* 1999). It is important to choose proper values of h and S in siphon design based on the required critical shear stress in order to obtain good sediment cleansing.

CONCLUSIONS

An experimental investigation on the flow field and sediment scour on the bottom of the overflow chamber is presented, and the hydraulic behavior and sediment removal effectiveness of the SSCS are analyzed and discussed. The results show that the velocity and shear stress distribution in the chamber decreased rapidly at first and then gradually stabilized as the horizontal distance between the measurement point and the suction head increased. In the vertical direction, the shear stress and velocity decreased rapidly. The siphon suction improved the overall hydraulic behavior in the chamber, and was helpful for preventing excessive sediment accumulation in the overflow chamber. The sediment scour test revealed that the equilibrium scour depth was correlated significantly with the siphon-lift capacity of the SSCS. A larger siphon-lift capacity of the SSCS can result in a deeper sediment scour. The siphon-lift capacity, which can be expressed by $\bar{\tau}$, correlated significantly with the value of h and S. The initial hydraulic head, h, is the requisite condition for the adoption of SSCS. Further research is needed on the effect of the suction head type, installation angle and height of SSCS on sediment removal.

ACKNOWLEDGEMENTS

The project was supported by the Special Grand National Science-Technology Project for Water Pollution Control and Treatment, China (No. 2008ZX07317-001) and the National Nature Science Foundation of China (No. 50908070)

REFERENCES

Ahyerre, M., Chebbo, G. & Saad, M. 2001 Nature and dynamics of water sediment interface in combined sewers. *Journal of Environmental Engineering* **127** (3), 233–239.

Ashley, R. M., Bertrand-Krajewski, J. L., Hvited-Jacobsen, T. & Verbanck, M. 2004 *Solids in Sewers: Characteristics, Effects and Control of Sewer Solids and Associated Pollutants*. IWA Publishing, London, UK.

Ashley, R. M., Fraser, A., Burrows, R. & Blanksby, J. 2000 The management of sediment in combined sewers. *Urban Water* **2** (4), 263–275.

Bertrand-Krajewski, J.-L. 2003 Sewer sediment management: some historical aspects of egg shape sewers and flushing tanks. *Water Science and Technology* **47** (4), 109–122.

Bertrand-Krajewski, J. L., Campisano, A., Creaco, E. & Modica, C. 2004 Experimental study and modelling of the hydraulic behaviour of a Hydrass flushing gate. *Proceedings of Novatech 2004, Fifth International Conference on Sustainable Techniques and Strategies in Urban Water Management*, 6–10 June, Lyon, France.

Campisano, A., Creaco, E. & Modica, C. 2006 Experimental analysis of the hydrass flushing gate and laboratory validation of flush propagation modelling. *Water Science and Technology* **54** (6–7), 101–108.

Campisano, A., Creaco, E. & Modica, C. 2007 Dimensionless approach for the design of flushing gates in sewer channels. *Journal of Hydraulic Engineering* **133** (8), 964–972.

Campisano, A., Creaco, E. & Modica, C. 2008 Laboratory investigation on the effects of flushes on cohesive sediment beds. *Urban Water Journal* **5** (1), 3–14.

Chebbo, G., Laplace, D., Bachoc, A., Sanchez, Y. & Le Guennec, B. 1996 Technical solutions envisaged in managing solids in combined sewer networks. *Water Science and Technology* **33** (9), 237–244.

Chen, S. C., Wang, S. C. & Wu, C. H. 2010 Sediment removal efficiency of siphon dredging with wedge-type suction head and float tank. *International Journal of Sediment Research* **25** (2), 149–160.

Dufresne, M., Vazquez, J., Terfous, A., Ghenaim, A. & Poulet, J. B. 2009 Experimental investigation and CFD modelling of flow, sedimentation, and solids separation in a combined sewer detention tank. *Computers & Fluids* **38**, 1042–1049.

Harwood, R. & Saul, A. J. 2001 Modelling the performance of combined-sewer overflow chambers. *Journal of the Chartered Institution of Water and Environmental Management* **15**, 300–304.

Pisano, W. C., Barsanti, J., Joyce, J. J. & Sorensen, H. J. 1998 Sewer and tank sediment flushing: Case studies. Rep. No. EPA/625/R-98/157 (NTIS PB 99–127839), US Environmental Protection Agency, National Risk Management Research Laboratory, Cincinnati, OH, USA.

Pisano, W. C., O'Riordan, O. C., Ayotte, F. J., Barsanti, J. R. & Carr, D. L. 2003 Automated sewer and drainage flushing systems in Cambridge, Massachusetts. *Journal of Hydraulic Engineering* **129** (4), 260–266.

Skipworth, P. J., Tait, S. J. & Saul, A. J. 1999 Erosion of sediment beds in sewers: model development. *Journal of Environmental Engineering* **125** (6), 566–573.

Stovin, V. R. & Saul, A. J. 2000 Computational fluid dynamics and the design of sewage storage chambers. *Journal of the Chartered Institution of Water and Environmental Management* **14**, 103–110.

First received 17 September 2012; accepted in revised form 4 March 2013